Error Estimates for Near-Real-Time Satellite Soil Moisture as Derived From the Land Parameter Retrieval Model

Robert M. Parinussa, Antoon G. C. A. Meesters, Yi Y. Liu, Wouter Dorigo, Wolfgang Wagner, and Richard A. M. de Jeu

***Abstract*—A time-efficient solution to estimate the error of satellite surface soil moisture from the land parameter retrieval model is presented. The errors are estimated using an analytical solution for soil moisture retrievals from this radiative-transfer-based model that derives soil moisture from low-frequency passive microwave observations. The error estimate is based on a basic error propagation equation which uses the partial derivatives of the radiative transfer equation and estimated errors for each individual input parameter. Results similar to those of the Monte Carlo approach show that the developed time-efficient methodology could substitute computationally intensive methods. This procedure is therefore a welcome solution for near-real-time data assimilation studies where both the soil moisture product and error estimate are needed. The developed method is applied to the C-, X-, and Ku-bands of the Aqua/Advanced Microwave Scanning Radiometer for Earth Observing System sensor to study differences in errors between frequencies.**

***Index Terms*—Analytical solution, error analysis, passive microwave, radiative transfer, soil moisture.**

I. Introduction

With the recent changes in data distribution, it is currently possible to produce satellite soil moisture from the Advanced Microwave Scanning Radiometer for Earth Observing System (AMSR-E) microwave sensor with latency of approximately 2 h from the satellite observation [22]. Numerous data assimilation studies (e.g., [1] and [6]) demonstrated the need of additional satellite soil moisture error estimates to improve weather and flood forecasts. Ideally, we would like to produce soil moisture and its associated error estimate simultaneously. Unfortunately, statistical error propagation methods, like the Monte Carlo simulation, are computationally intensive, thus minimizing the possibility to produce soil moisture error estimates in a near-real-time mode. This letter presents an analytical solution that aims to derive soil moisture error estimates from satellite observations with a minimum computing time; this creates the opportunity to simultaneously calculate both the soil moisture and the associated error.

Different soil moisture data sets derived from passive microwave observations are available (e.g., [9], [16], and [18]), but until now, none of them produces the associated soil moisture errors next to the soil moisture values in an automated fashion. However, in the active field, this is already a common practice [15]. Recently, Liu *et al.* [11] have shown that the combination of passive- and active-microwave-based soil moisture data sets has the potential to provide higher quality soil moisture product compared to single-sensor data sets. Estimation of associated errors for the soil moisture product derived from passive microwave observations could lead to a more solid combination strategy, particularly on a shorter timescale (near real time).

One of the more promising passive microwave soil moisture products is based on the land parameter retrieval model (LPRM) [18]. This model uses a simple radiative transfer equation to obtain soil moisture from microwave observations and has an accuracy of about 0.06 $m^3 \cdot m^{-3}$ for sparsely to moderately vegetated regions [2]. Due to the simple nature of this model, we assigned this model to derive an analytical solution to estimate the soil moisture errors. The LPRM has been applied to C-, X-, and Ku-band satellite observations and uses an optimization technique to extract soil moisture and vegetation optical depth from horizontally and vertically polarized microwave brightness temperatures by partitioning the observed signal into its respective soil and vegetation emission components [3], [12], [18]; surface soil temperature is estimated offline with a separate retrieval algorithm [7]. Several studies have shown the agreement between *in situ* soil moisture observations and LPRM-based soil moisture retrievals (e.g., [2] and [23]). Dorigo *et al.* [5] explored the relative uncertainty of globally available LPRM soil moisture products using the triple collocation error estimation technique. Miralles *et al.* [13] investigated the uncertainties resulting from the scale mismatch between pointlike observations and satellite footprint scale. All methods give us information on the quality of the soil

Manuscript received November 23, 2010; revised February 8, 2011; accepted February 9, 2011. This work was supported in part by the Support to Science Element of the European Space Agency's Earth Observation Programme (EOEP-STSE-EOPG-SW-08-0001) as part of the Water Cycle Multimission Observation Strategy project (European Space Research Institute/Contract 22086/08/I-EC) coordinated by the International Institute of Geo-Information Science and Earth Observation (ITC) and in part by the National Aeronautics and Space Administration Research Opportunities in Space and Earth Sciences (NNH08ZDA001N).

R. M. Parinussa, A. G. C. A. Meesters, and R. A. M. de Jeu are with the Department of Hydrology and Geo-Environmental Sciences, Faculty of Earth and Life Sciences, Vrije Universiteit Amsterdam, 1081 HV Amsterdam, The Netherlands (e-mail: Robert.Parinussa@falw.vu.nl; Antoon.Meesters@falw.vu.nl; Richard.de.Jeu@falw.vu.nl).

Y. Y. Liu is with the School of Civil and Environmental Engineering, University of New South Wales, Sydney, N.S.W. 2052, Australia, and also with the Commonwealth Scientific and Industrial Research Organisation Land and Water, Canberra, A.C.T. 2601, Australia (e-mail: Yi.Y.Liu@csiro.au).

W. Dorigo and W. Wagner are with the Institute of Photogrammetry and Remote Sensing, Vienna University of Technology, 1040 Vienna, Austria (e-mail: wd@ipf.tuwien.ac.at; ww@ipf.tuwien.ac.at).

Color versions of one or more of the figures in this paper are available online at http://ieeexplore.ieee.org.

Digital Object Identifier 10.1109/LGRS.2011.2114872

moisture products, but *in situ* analysis only gives us information for the studied regions, while the triple collocation method does not give us error estimates of the individual observations. Statistical approaches (e.g., Monte Carlo) can be used [15] to estimate the error of LPRM-based soil moisture retrievals but are computationally intensive because many iterative model runs are needed to derive statistically reliable error estimates. Because of the high computational cost of the Monte Carlo approach, it is impractical to apply such a technique in an operational fashion.

To overcome these issues, an analytical solution to estimate the error of LPRM surface soil moisture was derived. The analytical error estimation is based on a basic error propagation equation which uses the partial derivatives of the radiative transfer equation and estimated errors for each individual input parameter to calculate the standard deviation in the dielectric (k) constant. This standard deviation can be used to determine the error in the soil moisture retrieval using a dielectric mixing model [24] under the assumption that the dielectric mixing model itself is correct. The analytical error estimate provides the random error of the soil moisture product, at the right time and spatial scale, which can be explained from the retrieval method (the radiative transfer equation).

II. Materials and Models

A. Passive Microwave Observations

The AMSR-E is a sensor on board the National Aeronautics and Space Administration's Aqua satellite which was launched on May 4, 2002. The satellite orbits the Earth at an altitude of 705 km and scans with an incidence angle of 55°. Observations are made in vertical (V) and horizontal (H) polarizations at six frequencies, of which four are relevant for soil moisture retrievals. The spatial resolutions of the C-, X-, Ku-, and Ka-band observations are 73 × 43 km, 51 × 30 km, 27 × 16 km, and 14 × 8 km, respectively. For more detailed information on the Aqua/AMSR-E sensor, readers are directed to [17]. The Aqua/AMSR-E makes both daytime and nighttime observations; only nighttime observations are used in this letter as it was shown that soil moisture retrievals based on these are more reliable than those based on daytime observations [2]. Moreover, this letter only considers brightness temperature observations for the year 2008, which we resampled to a 0.25° global grid.

B. LPRM

The retrieval methodology uses a radiative transfer equation in two polarizations to solve for soil moisture and vegetation optical depth simultaneously using a nonlinear iterative optimization procedure. Mo *et al.* [14] provides the radiative transfer

$$T_{b(P)} = T_S e_{r(P)} \Gamma + (1-\omega) T_C (1-\Gamma) + \left(1 - e_{r(P)}\right)(1-\omega) T_C (1-\Gamma)\Gamma \quad (1)$$

where T_b refers to the observed brightness temperatures, P refers to either H or V polarization, T_S and T_C are the thermometric temperatures of the soil and the canopy, respectively, e_r refers to the rough surface emissivity, ω is the single scattering albedo, and the transmissivity (Γ) is defined in terms of the optical depth (τ) according to (2), where u refers to the incidence angle

$$\Gamma = \exp\left(\frac{-\tau}{\cos(u)}\right). \quad (2)$$

The land surface temperature (T_{LS}) is assumed to be the area mean of T_S and T_C, is derived from the Ka-band vertically polarized brightness temperature [7], and is calculated external to the retrieval algorithm. A more detailed description of the soil moisture retrieval model may be found in [18]. Some well-known limitations in the retrieval model require a masking routine to be implemented. This masking routine eliminates data where values are meaningless, such as areas with snow cover or frozen surface conditions [7] or areas with radio-frequency interference [10].

TABLE I
Input Parameters and Associated Error

Input parameter	Symbol	Input value	Associated error
Brightness temperature C-band	Tb	Observation	0.3 K
Brightness temperature X-band	Tb	Observation	0.6 K
Brightness temperature Ku-band	Tb	Observation	0.6 K
Land surface temperature	T_{LS}	Retrieved parameter	1.8 – 2.5 K
Empirical roughness parameter	h	0.18	0.018
Cross polarization	Q	0.127	0.0127
Single scattering albedo	ω	0.05	0.005

C. Errors of Input Parameters

Some input parameters, like brightness temperature observations, have well-defined values for their accuracy, while for others, it is only possible to provide an estimate. The sensor sensitivity for the AMSR-E sensor is a well-known value; for C-band brightness temperature observations, it is 0.3 K, and for the other bands relevant for soil moisture retrieval (X- and Ku-bands), it is 0.6 K [17]. Moreover, the land surface temperature algorithm has been extensively validated (e.g., [7] and [21]) with an error value varying between 2.5 K for nonvegetated to lowly vegetated areas and 1.8 K for highly vegetated areas for AMSR-E nighttime observations; these values include the AMSR-E Ka-band sensor sensitivity of 0.6 K.

Other input parameters do not have well-defined values for their accuracy because it is often difficult to derive a reliable estimate. Limitations on measuring techniques, high spatial and temporal variability, and problems due to upscaling of parameters may all contribute to this error. The LPRM uses single global values for the single scattering albedo (ω) and the roughness parameters (h and Q). In a recent study, de Jeu *et al.* [4] demonstrated that a complex parameterization is not necessary to improve soil moisture retrieval capabilities; therefore, we choose to solely use fixed values for ω, h, and Q. The associated error for the parameters where it is only possible to provide an estimate was chosen to be 10% of its input value; this noise value is rather arbitrary but a commonly used value for error analysis [15]. Table I shows the input parameters and their associated error estimates that were used to compare the analytical error propagation and the Monte Carlo simulation.

III. Analytical Derivation

In this section, the radiative transfer (1) is rewritten, and an analytical solution for the standard deviation in the dielectric constant (k) is derived. The basis of the analytical solution to calculate the error in soil moisture lies in the use of a basic error propagation

$$S_{\text{obs}} = J S_{\text{mod}} J^{\text{T}} \tag{3}$$

where S_{obs} and S_{mod} are the covariance matrices for the observation and model parameters, respectively, J is the Jacobian matrix (4), and T denotes the transpose. J is used for the transformation from the model parameters $(\Gamma, k, T_{\text{LS}}, \omega, h)$ to the observations and estimations $(T_{\text{bH}}, T_{\text{bV}}, T_{\text{LS,obs}}, \omega_{\text{est}}, h_{\text{est}})$

$$J = \begin{pmatrix} \frac{\partial T_{\text{bH}}}{\partial \Gamma} & \frac{\partial T_{\text{bH}}}{\partial k} & \frac{\partial T_{\text{bH}}}{\partial T_{\text{LS}}} & \frac{\partial T_{\text{bH}}}{\partial \omega} & \frac{\partial T_{\text{bH}}}{\partial h} \\ \frac{\partial T_{\text{bV}}}{\partial \Gamma} & \frac{\partial T_{\text{bV}}}{\partial k} & \frac{\partial T_{\text{bV}}}{\partial T_{\text{LS}}} & \frac{\partial T_{\text{bV}}}{\partial \omega} & \frac{\partial T_{\text{bV}}}{\partial h} \\ 0 & 0 & 1 & 0 & 0 \\ 0 & 0 & 0 & 1 & 0 \\ 0 & 0 & 0 & 0 & 1 \end{pmatrix}. \tag{4}$$

The methodology is adapted to determine the variance σ_k^2 of the dielectric constant (k). It was chosen to determine the variance of the dielectric constant (k) because it is the principal observation. Another reason to determine the variance of the dielectric constant (k) is the existence of several different models linking the dielectric constant (k) to soil moisture. Based on the findings by Owe and van de Griend [20], we use the dielectric mixing model of Wang and Schmugge [24] to link the variance of the dielectric constant (k) to the error estimate in soil moisture. The challenge in using the basic error propagation methodology (3) is to define the partial derivatives. To define the partial derivatives, we used the Jacobian matrix (4), which is a matrix containing the first-order partial derivatives of the radiative transfer equation with respect to each variable.

The radiative transfer (1) was rewritten and reorganized to (5); for convenience, we drop subscript "P" for polarization

$$T_b = T_{\text{LS}} \left[e_r \left(\Gamma - (1-\omega)(1-\Gamma)\Gamma \right) + (1-\omega)(1-\Gamma^2) \right]. \tag{5}$$

For convenience, the expressions $F(\Gamma, \omega)$ (6) and $G(\Gamma, \omega)$ (7) are defined to rewrite (5), resulting in (8)

$$F(\Gamma, \omega) = \Gamma - (1-\omega)(1-\Gamma)\Gamma \tag{6}$$
$$G(\Gamma, \omega) = (1-\omega)(1-\Gamma^2) \tag{7}$$
$$T_b = T_{\text{LS}} \left[F(\Gamma, \omega) e_r(k, h) + G(\Gamma, \omega) \right]. \tag{8}$$

The rough surface emissivity $e_{r(P)}$ follows from (9), where the polarization is reintroduced. This equation was written to calculate the rough surface emissivity in H polarization. To calculate the rough surface emissivity in V polarization, the (H) and (V) signs should swap. Q is the roughness parameter known as the cross polarization, and h is the roughness

$$e_{r(H)}(k, h) = 1 - \left\lfloor Q \left(1 - e_{s(V)}(k) \right) + (1-Q) \left(1 - e_{s(H)}(k) \right) \right\rfloor \chi(h) \tag{9}$$

where the last term refers to

$$\chi(h) = \exp\left(-h \cdot \cos(u) \right). \tag{10}$$

The smooth surface emissivity was calculated using (11) and (12); for convenience, we drop subscript "s" from the smooth emissivity

$$e_H = 1 - \left(\frac{\cos(u) - \Delta}{\cos(u) + \Delta} \right)^2 \tag{11}$$
$$e_V = 1 - \left(\frac{k \cdot \cos(u) - \Delta}{k \cdot \cos(u) + \Delta} \right)^2 \tag{12}$$

where the Δ term refers to

$$\Delta = \sqrt{k - \sin^2 u}. \tag{13}$$

The following derivatives will be needed:

$$\frac{\partial F}{\partial \Gamma} = 1 - (1-\omega)(1-2\Gamma) \tag{14}$$
$$\frac{\partial G}{\partial \Gamma} = -2(1-\omega)\Gamma \tag{15}$$
$$\frac{\partial e_H}{\partial k} = \frac{2\cos(u)}{\Delta} \frac{\cos(u) - \Delta}{(\cos(u) + \Delta)^3} \tag{16}$$
$$\frac{\partial e_V}{\partial k} = 2\cos(u) \left(\frac{k}{\Delta} - 2\Delta \right) \frac{k \cdot \cos(u) - \Delta}{(k \cdot \cos(u) + \Delta)^3}. \tag{17}$$

From these equations, it follows that the Jacobian matrix (4) can be calculated analytically. The numbers subscripted in J represent locations in the Jacobian matrix $(J_{\text{row,column}})$

$$J_{11} = T_{\text{LS}} \left(\frac{\partial F}{\partial \Gamma} e_{r,H} + \frac{\partial G}{\partial \Gamma} \right) \tag{18}$$
$$J_{21} = T_{\text{LS}} \left(\frac{\partial F}{\partial \Gamma} e_{r,V} + \frac{\partial G}{\partial \Gamma} \right) \tag{19}$$
$$J_{12} = T_{\text{LS}} F \left(Q \frac{\partial e_V}{\partial k} + (1-Q) \frac{\partial e_H}{\partial k} \right) \chi \tag{20}$$
$$J_{22} = T_{\text{LS}} F \left(Q \frac{\partial e_H}{\partial k} + (1-Q) \frac{\partial e_V}{\partial k} \right) \chi \tag{21}$$
$$J_{13} = F e_{r,H} + G \tag{22}$$
$$J_{23} = F e_{r,V} + G \tag{23}$$
$$J_{14} = T_{\text{LS}} \left[(1-\Gamma)\Gamma e_{r,H} - 1 + \Gamma^2 \right] \tag{24}$$
$$J_{24} = T_{\text{LS}} \left[(1-\Gamma)\Gamma e_{r,V} - 1 + \Gamma^2 \right] \tag{25}$$
$$J_{15} = T_{\text{LS}} F \left[Q(1-e_V) + (1-Q)(1-e_H) \right] \chi \cos(u) \tag{26}$$
$$J_{25} = T_{\text{LS}} F \left[Q(1-e_H) + (1-Q)(1-e_V) \right] \chi \cos(u). \tag{27}$$

It follows that the variations in the observed and estimated parameters $(T_{\text{bH}}, T_{\text{bV}}, T_{\text{LS,obs}}, \omega_{\text{est}}, h_{\text{est}})$ are related to the variations in the model parameters $(\Gamma, k, T_{\text{LS}}, \omega, h)$; this results in the following expression:

$$S_{\text{mod}} = J^{-1} S_{\text{obs}} (J^{-1})^{\text{T}}. \tag{28}$$

Working out $S_{\text{mod},22}$ yields (29), where the correlation between the errors in T_{bH} and T_{bV} is expressed in r

$$\begin{aligned} \sigma_k^2 = & \left((J^{-1})_{21} \right)^2 \sigma_{\text{TbH}}^2 + \left((J^{-1})_{22} \right)^2 \sigma_{\text{TbV}}^2 \\ & + 2 \left((J^{-1})_{21} \right) \left((J^{-1})_{22} \right) r \sigma_{\text{TbH}} \sigma_{\text{TbV}} \\ & + \left((J^{-1})_{23} \right)^2 \sigma_{\text{LS(obs)}}^2 + \left((J^{-1})_{24} \right)^2 \sigma_{\omega}^2 \\ & + \left((J^{-1})_{25} \right)^2 \sigma_h^2. \end{aligned} \tag{29}$$

To compare the analytical solution to the traditional Monte Carlo simulation and to study the differences in errors between frequencies, we selected several *in situ* test locations $(n = 107)$

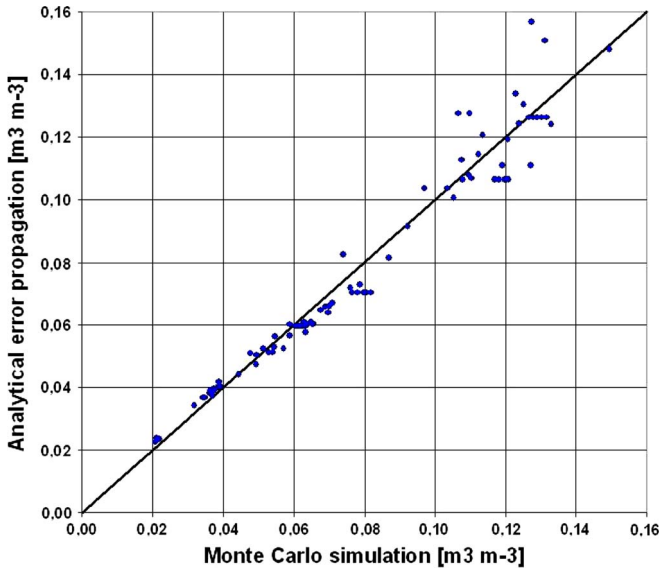

Fig. 1. Scatter plot of the average error estimates from the Monte Carlo simulation against the error estimates of the analytical error propagation.

worldwide (Australia, Spain, France, Mali, and the U.S.) representing a large variety of land covers and vegetation densities. Identical input data (C-band observations) and error estimates (Table I) were used in the traditional Monte Carlo simulation and the analytical error propagation to estimate the error in the soil moisture product.

IV. Results

To compare the results obtained from both methods, the averaged error estimates using the analytical error propagation $(\mathrm{m}^3 \cdot \mathrm{m}^{-3})$ were plotted against the averaged error estimates using the Monte Carlo simulation $(\mathrm{m}^3 \cdot \mathrm{m}^{-3})$ (Fig. 1). There is a high correlation $(R = 0.96)$ between the error estimates obtained from the Monte Carlo simulation and the analytical error propagation. The high correlation and the close match to the one-to-one line show that there is good agreement between both methods.

For the same locations and time period, the analytical error was estimated for three different microwave frequencies (C-, X-, and Ku-bands). Results (Fig. 2) show larger error values in the retrieved soil moisture product for higher frequencies at similar vegetation optical depth values. For example, for a specific agricultural crop $(vegetation\ optical\ depth = 0.5)$, the error estimate for the soil moisture retrieval in the C-band is around 0.07 $\mathrm{m}^3 \cdot \mathrm{m}^{-3}$; in the X-band, this is around 0.11 $\mathrm{m}^3 \cdot \mathrm{m}^{-3}$, and in the Ku-band, this is around 0.16 $\mathrm{m}^3 \cdot \mathrm{m}^{-3}$. All relevant frequency bands show an increasing error with increasing vegetation optical depth. This is consistent with theoretical predictions, which indicate that, as the vegetation biomass increases, the observed soil emission decreases, and therefore, the soil moisture information contained in the microwave signal decreases [2]. In addition, the higher frequency retrievals (i.e., X- and Ku-bands) are adversely influenced by a much thinner vegetation cover.

To show the temporal behavior of the analytical error estimate, a time series for three different locations in the Sahel region is presented (Fig. 3). The Sahel region was chosen because

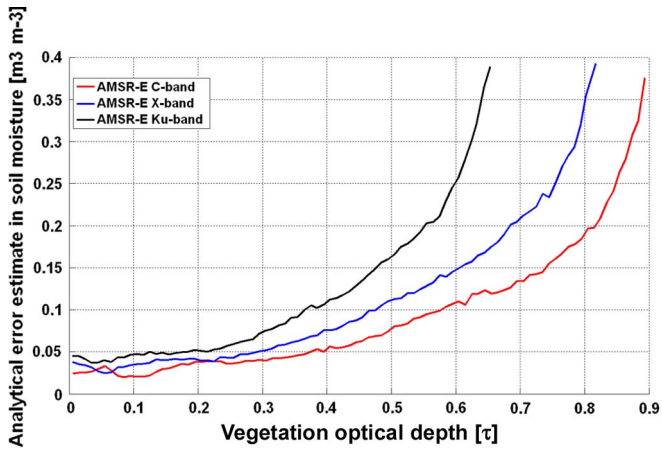

Fig. 2. Error of soil moisture as related to the vegetation optical depth for three different frequency bands.

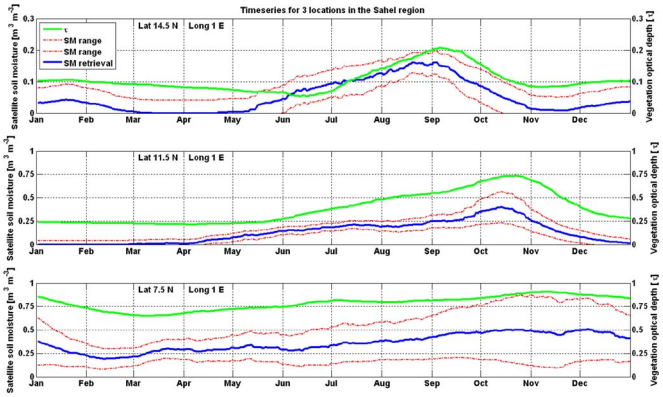

Fig. 3. Time series for three different locations in the Sahel region. Note the different scale in the upper time series.

there is a strong transition between dry and nonvegetated to lowly vegetated areas (upper) in the north and wet and densely vegetated areas (lower) in the south. Also, there is a strong seasonal variation (middle) in the transition zone between these two. The figure represents the 30-day central moving average of the presented parameters. The error estimate is added and subtracted from the associated soil moisture retrieval and is represented by the range. It was shown that the analytical error estimates in the dry and lowly vegetated regions are low and consistent in time. In the transition zone, a similar behavior is observed in the beginning of the time series. Strong changes in vegetation are observed from September onward; comparable behavior is observed for the error estimate. In the wet and densely vegetated areas, it is shown that the analytical error estimates are high and show comparable behavior when the vegetation density decreases (February–March period).

The presented error propagation method is applied on a global scale to all descending AMSR-E C-band observations for the year 2008. Daily global error estimate maps were averaged into a yearly representation (Fig. 4). Spatial patterns show strong connection to the global vegetation distribution. In tropical regions and boreal forests, which are characterized with dense vegetation, the error estimate is high. Savanna and tundra show intermediate error estimates, and in desert regions, the error estimates are low.

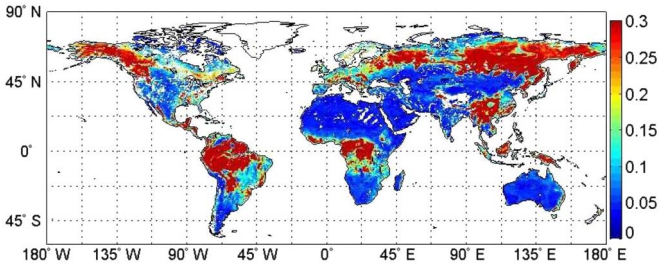

Fig. 4. Global representation of the soil moisture error estimates $(\mathrm{m}^3 \cdot \mathrm{m}^{-3})$ for the AMSR-E C-band observations.

V. Discussion and Conclusion

The methodology presented in this letter has shown that it is possible to provide an analytical solution to derive soil moisture error estimates from satellite observations. This creates the opportunity to produce satellite soil moisture and estimate the associated error of the satellite soil moisture product in near real time. Applying the analytical error propagation method shows results that are in line with the theory. This theory states that, at higher microwave frequencies, the error of a retrieved soil moisture value at similar optical depth values is generally higher. Single-frequency observations show increasing error estimates at higher optical depth values. Similar results for the Monte Carlo simulation and the analytical error propagation suggest that the time-efficient analytical solution can replace the computationally intensive Monte Carlo simulation. The spatial patterns of the analytical error estimate correspond well to the spatial patterns obtained by the triple collocation technique [5], while the patterns observed by both methods show a strong connection to vegetation distribution. More research is needed to investigate the results of the analytical error propagation method particularly to validate absolute values of the analytical error estimation. It is suggested to use triple collocation and comparisons with *in situ* soil moisture observations for this validation.

Most recent [Soil Moisture and Ocean Salinity (SMOS)] and future satellite missions [Aquarius and Soil Moisture Active and Passive (SMAP)] will make observations in lower microwave frequencies (1.4 GHz; L-band). Because of the better signal-to-noise ratio in this frequency, observations are expected to be more sensitive to soil moisture. Unfortunately, SMOS and SMAP lack an additional sensor to simultaneously sense land surface temperature, and the associated error in the brightness temperature observations is higher than that in the AMSR-E observations. The methodology presented in this letter can account for all these factors, and therefore, the basic principle could be used for L-band satellite observations.

With the current availability of AMSR-E satellite brightness temperatures with a latency of $\sim$2 h behind observations and the described analytical solution, it is possible to produce simultaneously the soil moisture and the associated error estimate in near real time. It is expected that these near-real-time data streams will be available for user download via the Goddard Earth Sciences Data and Information Services Center.

References

[1] L. Brocca, F. Melone, T. Moramarco, W. Wagner, V. Naeimi, Z. Bartalis, and S. Hasenauer, "Improving runoff prediction through the assimilation of the ASCAT soil moisture product," *Hydrol. Earth Syst. Sci.*, vol. 14, no. 10, pp. 1881–1893, Oct. 2010.

[2] R. A. M. de Jeu, W. Wagner, T. R. H. Holmes, A. J. Dolman, N. C. van de Giesen, and J. Friesen, "Global soil moisture patterns observed by space borne microwave radiometers and scatterometers," *Surveys Geophys.*, vol. 29, no. 4/5, pp. 399–420, Oct. 2008.

[3] R. A. M. de Jeu and M. Owe, "Further validation of a new methodology for surface moisture and vegetation optical depth retrieval," *Int. J. Remote Sens.*, vol. 24, no. 22, pp. 4559–4578, Nov. 2003.

[4] R. A. M. de Jeu, T. R. H. Holmes, R. Panciera, and J. P. Walker, "Parameterization of the land parameter retrieval model for L-band observations using the NAFE'05 dataset," *IEEE Geosci. Remote Sens. Lett.*, vol. 6, no. 4, pp. 630–634, Oct. 2009.

[5] W. Dorigo, K. Scipal, R. M. Parinussa, Y. Y. Liu, W. Wagner, R. A. M. de Jeu, and V. Naeimi, "Error characterisation of global active and passive microwave soil moisture data sets," *Hydrol. Earth Syst. Sci.*, vol. 14, pp. 2605–2616, 2010.

[6] M. Drusch, "Initializing numerical weather prediction models with satellite-derived surface soil moisture," *J. Geophys. Res. Atm.*, vol. 112, no. 3, p. D03102, Feb. 2010.

[7] T. R. H. Holmes, R. A. M. de Jeu, M. Owe, and A. J. Dolman, "Land surface temperature from Ka band passive microwave observations," *J. Geophys. Res. Atm.*, vol. 114, no. D4, p. D04113, Feb. 2009.

[8] T. J. Jackson, T. J. Schmugge, and J. R. Wang, "Passive microwave sensing of soil moisture under vegetation canopy," *Water Resour. Res.*, vol. 18, no. 4, pp. 1137–1142, 1982.

[9] T. Koike, H. Fujii, T. Ohta, and E. Togashi, "Development and validation of TMI algorithms for soil moisture and snow," in *Proc. Remote Sens. Hydrol. 2000*, 2001, pp. 390–393, IAHS publ. no 267.

[10] L. Li, E. G. Njoku, E. Im, P. S. Chang, and K. S. Germain, "A preliminary survey of radio-frequency interference over the U.S. in Aqua AMSR-E data," *IEEE Trans. Geosci. Remote Sens.*, vol. 42, no. 2, pp. 380–390, Feb. 2004.

[11] Y. Y. Liu, R. M. Parinussa, W. Dorigo, R. A. M. de Jeu, W. Wagner, A. I. J. M. van Dijk, M. F. McCabe, and J. P. Evans, "Developing an improved soil moisture dataset by blending passive and active microwave satellite-based retrievals," *Hydrol. Earth Syst. Sci.*, vol. 15, no. 2, pp. 425–436, Feb. 2011.

[12] A. G. C. A. Meesters, R. A. M. de Jeu, and M. Owe, "Analytical derivation of the vegetation optical depth from the microwave polarization difference index," *IEEE Geosci. Remote Sens. Lett.*, vol. 2, no. 2, pp. 121–123, Apr. 2005.

[13] D. G. Miralles, W. Crow, and M. Cosh, "Estimating spatial sampling errors in coarse-scale soil moisture estimates derived from point-scale observations," *J. Hydrometeor.*, vol. 11, no. 6, pp. 1423–1429, Dec. 2010.

[14] T. Mo, B. J. Choudhury, T. J. Schmugge, J. R. Wang, and T. J. Jackson, "A model for microwave emission from vegetation-covered fields," *J. Geophys. Res.*, vol. 87, no. C13, pp. 11 229–11 237, 1982.

[15] V. Naeimi, K. Scipal, Z. Bartalis, S. Hasenauer, and W. Wagner, "An improved soil moisture retrieval algorithm for ERS and METOP scatterometer observations," *IEEE Trans. Geosci. Remote Sens.*, vol. 47, no. 7, pp. 1999–2013, Jul. 2009.

[16] E. G. Njoku, T. J. Jackson, V. Lakshmi, T. Chan, and S. V. Nghiem, "Soil moisture retrieval from AMSR-E," *IEEE Trans. Geosci. Remote Sens.*, vol. 41, no. 2, pp. 215–229, Feb. 2003.

[17] *National Snow and Ice Data Centre (NSIDC)*. Boulder, CO: Data Products and Services, 2006.

[18] M. Owe, R. A. M. de Jeu, and T. R. H. Holmes, "Multisensor historical climatology of satellite-derived global land surface moisture," *J. Geophys. Res. Earth Surf.*, vol. 113, p. F01 002, 2008.

[19] M. Owe, R. A. M. de Jeu, and J. P. Walker, "A methodology for surface soil moisture and vegetation optical depth retrieval using the microwave polarization difference index," *IEEE Trans. Geosci. Remote Sens.*, vol. 39, no. 8, pp. 1643–1654, Aug. 2001.

[20] M. Owe and A. A. van de Griend, "Comparison of soil moisture penetration depths for several bare soils at two frequencies and implications for remote sensing," *Water Resour. Res.*, vol. 34, no. 9, pp. 2319–2327, 1998.

[21] R. M. Parinussa, R. A. M. de Jeu, T. R. H. Holmes, and J. P. Walker, "Comparison of microwave and infrared land surface temperature products over the NAFE'06 research sites," *IEEE Geosci. Remote Sens. Lett.*, vol. 5, no. 4, pp. 783–787, Oct. 2008.

[22] K. Ramapriyan, J. Behnke, E. Sofinowski, D. Lowe, and M. Esfandiari, *Evolution of the Earth Observing System (EOS) Data and Information System (EOSDIS)*. New York: Springer-Verlag, 2010, pp. 63–92.

[23] W. Wagner, V. Naeimi, K. Scipal, R. A. M. de Jeu, and J. Martinez-Fernandez, "Soil moisture from operational meteorological satellites," *Hydrogeol. J.*, vol. 15, no. 1, pp. 121–131, Feb. 2007.

[24] J. R. Wang and T. J. Schmugge, "An empirical model for the complex dielectric permittivity of soils as a function of water content," *IEEE Trans. Geosci. Remote Sens.*, vol. GRS-18, no. 4, pp. 288–295, Oct. 1980.